

100-20-13-23
 HAZO 300 8-25
 HAZO 300 8-25

42

WORLDWIDE

RESEARCH PROGRAM ON APPLICATION OF
JET COMPRESSOR TO MAGNETOPLASMDYNAMIC
ELECTRICAL POWER GENERATION

Final Report

1 June 1963 - 30 November 1964

MND - 3176

MARTIN COMPANY
NUCLEAR DIVISION

MARTIN
MARIETTA 

RESEARCH PROGRAM ON APPLICATION OF
JET COMPRESSOR TO MAGNETOPLASMADYNAMIC
ELECTRICAL POWER GENERATION

Final Report

1 June 1963 - 30 November 1964

MND - 3176

RESEARCH PROGRAM ON APPLICATION OF JET COMPRESSOR
TO MAGNETOPLASMA DYNAMIC ELECTRICAL POWER GENERATION


Final Report

1 June 1963 - 30 November 1964

MND-3176

Order Number:	327
Project Code Number:	2980
Date of Contract:	1 June 1963
Contract Number:	Nonr-L087(00)
Contract Expiration Date:	30 November 1964
Project Scientist:	Dr. Cheng Shih, Phone 687-3800 Ext. 9315, Area Code 301
Contractor:	Martin Marietta Corporation Baltimore, Maryland 21203

Approved by:


W. J. Levedahl, Manager
Research
Nuclear Division

Martin Marietta Corporation
Baltimore 3, Maryland
December 1964

Reproduction in whole or in part is permitted for
any purpose of the United States Government.

Foreword

This report presents the work accomplished under contract Nonr-4087(00) for the period 1 June 1963 through 30 November 1964. The program was carried out under the auspices of the Advanced Research Project Agency and the Power Branch of the Office of Naval Research and was sponsored by Dr. J. Huth of ARPA and Mr. J. A. Satkowski of ONR.

Acknowledgement

The components in the experimental loop were designed by J. Goeller. Experimentation was carried out by E. N. Zavodny with assistance from W. Calary. W. Lyon worked out the equations for correlating experimental results to ideal ones and also the IBM computer code for such purpose.

TABLE OF CONTENTS

Foreword

Table of Contents

I. Introduction and Summary	
II. Analytical Studies	C. Shih
III. Experimental Procedures	E. Zavodny
IV. Results, Analysis and Discussion	C. Shih
V. Figures	
VI. Appendix	W. Lyon

I. INTRODUCTION AND SUMMARY

The objectives of this program are twofold: (1) to conduct an analysis and design study of a jet compressor based on a closed cycle in which the waste thermal energy available from an MPD system is transferred to a primary jet stream which compresses the MPD generator working medium; and (2) to design, fabricate and test a single stage jet compressor predicated on the results of the analysis and design study.

The program for achieving these two objectives had two main tasks; the first was analytical and the second predominantly experimental. The first task began with a relatively extensive literature search on the design and performance of jet compressors in general and ejectors for compressible flow in particular. Effort was directed to the analytical understanding of practical jet compressor performance. An IBM computer program was developed to study the performance of jet compressors with single and double-stage operations under prescribed flow distribution between stages. In each case, whether in single or multi-stage configuration, the waste thermal energy of an MPD power generator exhaust gas is used to power the compressor which, in turn, compresses the cooled exhaust gas. Results of the computation have shown that, with the available exhaust energy, a single stage jet compressor could provide a final-pressure-to-initial-pressure ratio (of the helium secondary stream) of about 1.5. With a two stage jet compressor, this ratio could be about 2.

The Semi-Annual Summary Technical Report⁽¹⁾, published January 1964, presented the derivation of ideal performance equations for a single-stage

jet compressor of the constant-area, mixing-chamber type, as well as modified equations which take into consideration the various efficiency coefficients. Also presented were the analysis and design of the various components of the experimental loop shown in Figure 1, as well as the engineering drawings. Except for direct reference purposes, this work will not be covered in this report.

In the second task, a closed loop test setup was designed, fabricated and installed. The test setup consists of a gaseous loop and a condensing-vapor loop. The gaseous loop contains helium saturated with cesium vapor and forms the secondary stream, simulating the working medium of an MPD power generator. In the condensing-vapor loop, pure cesium is vaporized, superheated and discharged under high pressure through a convergent-divergent nozzle to form the primary stream of the jet compressor. After mixing of the two streams and diffusion to low velocity, the cesium is then condensed, separated from the gas and pumped back to the boiler to repeat the cycle.

Fabrication and installation of the loop was completed by the end of September 1964. Leak checking and outgassing were completed by the first week of November 1964. During outgassing, the boiler wall was very gradually heated to 1300°K . Measurements of heat dissipation at various wall temperatures were taken to provide data for heater efficiency calculations. The heater efficiency thus calculated was about 90%.

A functional check of the components was made on 3 November 1964. Every component functioned smoothly. The first series of experimental runs were started on November 6, 1964 and the results obtained from that

series of runs were very encouraging. With the helium system at 0.245 atm, 633°K and with the cesium vapor at 6.45 atm, 1590°K, and flow rate of 8 gm/sec, the resulting performance was a helium pressure rise of 36% at a flow rate of 1.12 gm/sec.

A second performance test was undertaken on November 17, 1964 at a higher helium system pressure, about 0.18 atm. A pressure rise of 12% was obtained at a helium flow rate of 1.5 gm/sec. The primary stream cesium vapor was at 5.5 atm with a flow rate of 7.1 gm/sec. Both series of runs were made with a fixed mixing chamber length of 24 cm. The experimental results thus far obtained have been reasonably close to the expected values.

The results of the experimental runs on 6 November and 17 November have definitely established the feasibility of using a metallic vapor of high molecular weight to compress a gas of low molecular weight. The thermal efficiencies, about 10%, obtained in the preliminary runs confirmed the postulates of Martin ⁽²⁾ and the Pioneering Research Division of the Army Natick Laboratory ⁽³⁾.

SYMBOLS

A	cross sectional area, meter ²
C	specific heat, joules/kg-°K
F	force, Newtons
h	heat transfer coefficient, joules/M ² -sec-°K
H	enthalpy, joules/kg
L	length, m
\dot{m}	mass flow rate, Kg/sec
M*	critical Mach number, velocity/acoustic velocity at throat
p	pressure, Newton/m ²
R	gas constant, joules/Kg°K
T	temperature, °K
u	velocity of flow, m/sec
γ	ratio of specific heats
ρ	density, Kg/m ³

Subscript

e	exit
o	stagnation
p	constant pressure condition
v	constant volume condition
1	primary stream of jet compressor
2	secondary stream of jet compressor
3	conditions after mixing of the two streams

II. Analytical Study

An IBM 7094 digital computer program, based on the ideal performance equations originally developed at the Research Lab, was made for the parametric study of performance of jet compressors with one stage and two stages, respectively. In each case the energy required to power the compressor is derived from the waste heat energy in the exhaust from a model MPD power generator. The characteristic parameters of the generator are as follows:

Generator geometry:	constant cross-sectional area
Working medium, mol fraction	.99 He + .01 Cs
Stagnation temperature	2060°K
Mach number at generator inlet	0.45
Electrical loading factor $E/U_0 J_0$	0.8
Mach No. at generator exit	1.0
Area ratio of diffuser after generator	2.8
Pressure at generator inlet	0.5 atm
Pressure drop in system outside generator	0.25 atm
Exhaust temperature	1856°K

The jet compressor used to circulate the MPD generator working medium will use cesium vapor as the driving stream. It is assumed that the cesium which forms the primary stream of the jet compressor is heated up from condensate temperature to the saturation temperature, is vaporized, and is superheated in a heat exchanger by the exhaust heat from the MPD generator. The temperature drop across the heat exchanger wall is assumed to be 25°K.

A set of modified equations, taking into consideration the effects of non-ideal discharge coefficients, mixing efficiency, etc. was programmed as a basis for evaluating the experimental results. These computer programs were reported in the Semi-Annual Technical Report MND-3124 January 1964.

Results of computer runs indicated a possible pressure rise of 47% with single stage operation and a pressure rise of 97% with two stage operation using available exhaust heat from an assumed MPD generator. Both cases represent ideal conditions. The magnitude of the program did not permit computer calculations of three stage operation.

III. EXPERIMENTAL PROCEDURES

1. Experimental Setup

An experimental single stage jet compressor was designed, fabricated and operated. Superheated cesium vapor is discharged under high pressure through a convergent-divergent nozzle to form the primary stream. The secondary stream is composed of helium containing a small amount of cesium vapor to simulate the working medium of an MPD power generator. The compressed mixture is cooled in a condenser after passing through a diffuser, permitting separation and re-cycling of the cesium and helium. The various components of the system have been described in the first Semi-Annual Report, MND-3124. A block diagram of the jet compressor system and instrumentation is shown in Figure 1.

Pictures of a number of the important components of the loop are included in this report. Figure 2 shows the boiler-superheater unit in the welding fixture. The boiler is made of Nb-1% Zr alloy. It consists of two vertical concentric cylindrical shells. The cesium to be boiled is contained between the two cylindrical walls. Heat is supplied by means of radiation from an electrical resistance heater located inside of the inner boiler shell. The boiler heater, Figure 4, is made of Nb-1% Zr alloy tubing with knurled surfaces to increase surface emissivity. Similarly, the inner surface of the inner boiler shell was knurled for better radiation absorption.

The superheater, having a temperature range from 1400°K to 1800°K, is made of Ta-10% W alloy tubing and serves both as a vapor container and an electrical resistance heater itself. The superheater is in the form of a

coil to reduce the heat loss. Figure 3 shows the superheater coil before it was welded onto the boiler dome. Some difficulties were encountered in procuring this coil. The original vendor made three unsuccessful tries to electron-beam weld sheet stock and then draw it to size. The job was then turned over to National Research Corporation who used an extrusion process. An extrudable ring was first made from the ingot. The ring was then extruded and drawn to size by the Superior Tubing Company.

No information about coiling tubing of this alloy was available. It was finally coiled at the Zink Pipe Bending Company of Harrisburg, Pennsylvania under close supervision of Martin personnel. The coiling was done at room temperature since it appeared that no advantage would be obtained by heating to any temperature below that at which damaging oxidation might occur. Being previously annealed at 1700°K , the material was in a cold-workable condition with a hardness of Rockwell B-91. With a required coil ID of $3-1/8$ inches, the mandrel was sized at 3 inches to compensate for the $1/16$ inch radial spring-back.

Three compressor mixing chamber and diffuser sections were made for this experimental single stage unit, covering a range of mixing chamber lengths from 4" to 12". One section has a fixed mixing chamber length of 4 inches. The second one, having a variable mixing chamber length of 5 to $7-1/2$ inches, is shown in Figure 5. The section presently installed has a length range of $8-1/2$ to 12 inches. Experiments conducted to date have been with a length of $9-3/8$ inches.

2. Instrumentation

The essential instrumentation consists of pressure and temperature sensors at strategic points in the loop and a differential pressure, ori-

ifice type flow meter for helium flow-rate measurements. The helium static pressures at the nozzle (P_1 and P_2), the mixing chamber static pressure (P_3), the diffuser exit static pressure (P_4) and the helium flow differential pressure are detected by pneumatic transducers and continuously recorded on strip-chart recorders. The helium plenum, cesium pump outlet and superheater pressures are indicated by Bourdon gauges.

Temperatures measured using thermocouples are recorded on a multipoint recorder. Important temperatures measured include the boiler heater and wall temperatures (T_{18} and T_2), the cesium vapor temperature (T_{11}), the helium temperature at the nozzle (T_3), the mixing chamber temperature (T_4), and the plenum temperature (T_1). Thermocouples on the helium preheater and cesium preheater are used as input signals to controllers which maintain pre-set temperatures.

For temperature measurements below 1000°K in cesium atmosphere, chromel-alumel thermocouples in 316-SS sheaths are used. For temperatures above 1000°K , W-3% Re vs W-26% Re thermocouples are used. Bare thermocouples were preferred wherever possible and a dual installation was used for reliability. This proved fortunate, since the W-3% Re wire in one of the two bare thermocouples originally welded onto the boiler heater elements broke off when the heater was assembled. Since disassembly and reassembly are both risky and time consuming, the decision was made to operate with one thermocouple; it has been functioning nicely to date. With the data obtained during the outgassing period and during the experimental runs, even this thermocouple is no longer needed. Pt vs Pt-Rh thermocouples were not used for the intermediate temperature range since our experience indicated that this reacts with tantalum and columbium at that temperature

range when the materials are fused together. However, one Pt vs Pt-Rh couple is lightly spot welded to the boiler outer wall which is below 1400°K .

3. Loop Purification and Cesium Loading

All components of the loop were individually leak checked with a mass spectrometer leak detector. After assembly, the entire loop was thoroughly leak checked to insure leak tightness. It was then evacuated with a diffusion pump and all components of the loop were heated to their operating temperature or higher, with the exception of the superheater coil. Following this outgassing procedure, the loop was filled with helium to approximately one atmosphere of pressure and the helium was slowly circulated with the cesium pump. The impurity level was monitored with a gas chromatograph while the loop was again heated. No impurity buildup was detected.

Initially a 10 pound charge of cesium was loaded into the loop. It was first purified by heating to 400°C for 24 hours while in contact with a titanium sponge getter. This initial charge proved to be inadequate to operate the loop, and an additional 10 pound charge was loaded in 5 pound batches after purification in the same manner.

4. Experimentation

Two sets of runs have been made with the jet compressor loop, the first on 6 November 1964 and the second on 17 November 1964. The primary objective of these runs was to prove the principle of jet compressor operation with an alkali metal vapor as the driving fluid. A secondary objective was to obtain preliminary data for performance and efficiency analysis. Operation of the loop was satisfactory and both objectives were met.

During the first set of runs (Run A), the cesium boiler temperature (T_2) was brought up to 1060°K with a helium pressure of 0.50 atm abs, then increased to 1165°K (1640°F -- 72 psia) with a helium pressure of 0.25 atm abs. Data are listed in Table I. At the latter condition, the cesium vapor temperature at the superheater exit was calculated as 1590°K , while the cesium flow rate was 7.4 g/sec. The resultant performance was a helium pressure rise of 36% at a flow rate of 1.12 g/sec.

The reported cesium vapor temperature is that calculated from a heat balance because of inaccurate readings of the two thermocouples that had been installed to detect this temperature. There is also some uncertainty in the cesium flow rate, which is a function of the stroke length of the variable-stroke diaphragm type pump. The pump calibration may not be reliable.

The second set of runs (Run B) was carried out at a helium pressure of one-half atmosphere. The maximum boiler temperature was 1145°K . Other conditions were a cesium flow rate of 7.1 g/sec and cesium vapor temperature of 1318°K .

IV. ANALYSIS OF EXPERIMENTAL RESULTS

Data sheets for the preliminary test runs conducted on 6 November and 17 November 1964 are shown in Tables I and II. The helium flow rates and the four pressures (P_1 thru P_4) were recorded on strip charts. Analyses were made on a few steady-state runs, and the results are tabulated in Table III. Explanations are offered for some of the items.

1. Heat Loss from the Boiler and Superheater on Data Taken During the Outgassing Period

With no fluid circulation inside of the boiler and superheater, which were enclosed in a vacuum chamber, the total power to the heater must have been dissipated to the surroundings by radiation except for a very small fraction by conduction. During the outgassing period, the power consumption versus boiler wall temperature from 600°K up to 1300°K was recorded after an equilibrium condition was reached. The results are presented in Figure 10 in which the solid line represents the function

$$\text{Heat Loss} = \alpha T^4$$

For a known wall temperature, the radiation loss can be read from the curve immediately. However, the conditions are not entirely identical. In outgassing with no fluid in circulation, the boiler wall is at approximately uniform temperature and the heater is at a temperature only slightly higher. During experiments with circulation, the boiler wall has a temperature at the bottom equal to or less than that of the cesium at the preheater exit (T_5) and a temperature equal to the saturation temperature above the liquid level. An equivalent temperature

T_{Eff} bearing the relation

$$\int_0^A \beta T^4 dA = \beta AT_{\text{Eff}}^4$$

is used to find the heat dissipated to the surroundings. It is assumed that the temperature distribution on the boiler wall is uniform in all cases. It should be noted that the loss value thus obtained will be slightly less than the actual value because of the relatively higher heat loss through the circular bottom plate which is exposed to the higher temperature of the heater elements.

Heat loss from the superheater to the surroundings is treated in a similar manner. The same curve, using a correction factor to allow for the different surface of exposure, is used for the superheater since the insulation is identical in both cases.

2. Vapor Temperature

Due to the high degree of leak tightness required, the corrosiveness of one of the working media, and the high temperatures (up to 1800°K) required in this experiment, instrumentation was severely restricted in some areas. For example, any instrumentation that required a penetration became extremely difficult in the region between the boiler inlet and the superheater exit. Therefore, instrumentation in this area was kept to an absolute minimum. To determine the properties of the superheated vapor, two thermocouples of W - 3% Re vs. W-26% Re and one pressure probe were installed at the stagnation chamber just before the primary discharge nozzle. During the experiments, it was found that the two thermocouples

read temperatures apparently much lower than the actual. Thus, the vapor temperature is computed analytically from a heat balance. In this iterative technique, a vapor temperature is first assumed. The heat loss from the superheater surface at this vapor temperature is estimated according to the method described in IV.1. Then a heat balance is made to check whether the assumed vapor temperature rise is correct, and if not, another iteration is made.

3. Cesium Flow Rate

The diaphragm pump used for cesium circulation is a metering pump with a maximum capacity of 9.6 gph. When calibrated with water and alcohol, the pump was giving reproducible results whenever the pressure on the suction side exceeded 7 psia. Since the system was designed to operate at .25 atm abs, a cesium head of approximately .25 atm was provided between the reservoir and the pump suction side. However, during the experiments it was found that the discharge rate was not equal to the calibrated rate until the system pressure was increased to .5 atm abs. This was probably due to the unexpected flow resistance in the passage between the reservoir and the pump. Until a reliable flow meter is installed, it is necessary to calculate the cesium flow rate by other means. The cesium flow rates in the data analysis were calculated in two different ways; the results differed by a few per cent.

Knowing the boiler pressure (measured), the saturation temperature and the heat of vaporization can be found. From the boiler wall temperatures (measured), the heat dissipation to the ambient can be read from Figure 10 as was discussed in IV.1. Then the flow rate of cesium can be computed by

$$\text{Rate of vaporization} = \frac{\text{Net rate of heat supply to boiler}}{\text{Heat to raise liquid to saturation temperature} + \text{heat of vaporization}}$$

The flow rate thus calculated is entered in Table III under BOILER.

A check of this calculated value can be made by means of the flow through the primary stream discharge nozzle. The rate of flow through a critical nozzle (choked) can be calculated from the stagnation temperature and density of the flow medium. For a monatomic flow medium with stagnation temperature T_0 and stagnation pressure P_0 passing through a convergent-divergent nozzle of throat area A^* , the rate of discharge is:

$$\begin{aligned} \dot{m} &= \rho^* A^* u^* \\ &= \frac{.728 P_0 A^*}{\sqrt{R T_0}} \\ &= .092 \frac{P_0 A^*}{\sqrt{T_0}} \quad \text{Kg/sec for cesium vapor} \end{aligned}$$

If P_0' is the vapor pressure in atmospheres, the discharge rate is:

$$\dot{m} = .938 \times 10^{-4} \frac{P_0' A^*}{\sqrt{T_0}} \quad \text{Kg/sec}$$

The flow rate thus calculated is entered in Table III under SUPERHEATER. This flow rate should differ from that calculated from the boiler heat balance only by inaccuracies in temperature measurements.

4. Pressure Ratio of Compressor

The pressure ratio of the compressor is defined as the ratio of the pressure of the cesium-helium mixture at the exit of the diffuser (P_4) to

the initial helium pressure just before the secondary stream entrance (P_1). Both pressures P_4 and P_1 are measured by pneumatic pick-ups and recorded on strip chart recorders manufactured by the Swartout Division of the Crane Company. It was difficult to equalize the pressure level of the four recorders at any time. Therefore a calibration of the four recorders against the Bourdon gauge on the plenum had to be made and plotted before every series of test runs. The pressures recorded in Table III were values corrected against the calibrated results.

5. Compressor Efficiency

For jet compressors using gases for both primary and secondary streams, the efficiency may be given as the ratio of the isentropic enthalpy rise of the secondary stream to the isentropic enthalpy drop of the primary stream, i.e.

$$\eta_{Th} = \frac{\dot{m}_2 C_{p2} T_1 \left[\left(\frac{P_4}{P_1} \right)^{\frac{\gamma-1}{\gamma}} - 1 \right]}{\dot{m}_1 C_{p1} (T_{o1} - T_{o3})}$$

Results of efficiency calculated in this way are designated as thermal efficiency in Table III. The short coming of this definition, of course, is the neglect of the power required to raise the primary stream to the initial state. A more meaningful definition of efficiency may be defined as the ratio of the isentropic enthalpy rise of the secondary stream to the power supplied to the primary stream. In the case of vapor-driven compressors such as the cesium-helium compressor this report, the heat of vaporization should be also included. This cycle efficiency is given by:

$$\eta_{cy} = \frac{p_2 T_1 \left[\left(\frac{p_2}{p_1} \right)^{\frac{\gamma-1}{\gamma}} - 1 \right]}{\dot{m}_1 \left[H_v + C_{F1} (T_{o1} - T_{o3}) \right]}$$

where H_v is the heat of vaporization of the primary fluid. The pumping work to compress the liquid is negligibly small.

6. Discussion of Experimental Results

In both series of runs on November 6 and 17, 1964, the vapor was not superheated sufficiently to avoid condensation at the exit of primary nozzle. This was due to a malfunction of the vapor temperature thermocouple which caused concern about overheating the superheater coil. This problem can be precluded in the future by installation of a number of bare-wire thermocouples on the superheater wall.

Neglecting entirely the adverse effect due to condensation, the ideal compressor pressure ratio was calculated using actual experimental values of inlet temperatures, pressures and flow rates of the primary and secondary streams. The ratio of the actual measured pressure ratio to the ideal pressure ratio is defined as the effectiveness of the actual compressor. The effectiveness attained at a fixed compressor geometry in the two preliminary series of runs are listed in the last column of Table III. The 57% effectiveness attained in this preliminary feasibility run provides confidence that higher effectiveness may be obtained by optimization of operating conditions and compressor geometry.

JET COMPRESSOR - SIMPLIFIED SCHEMATIC

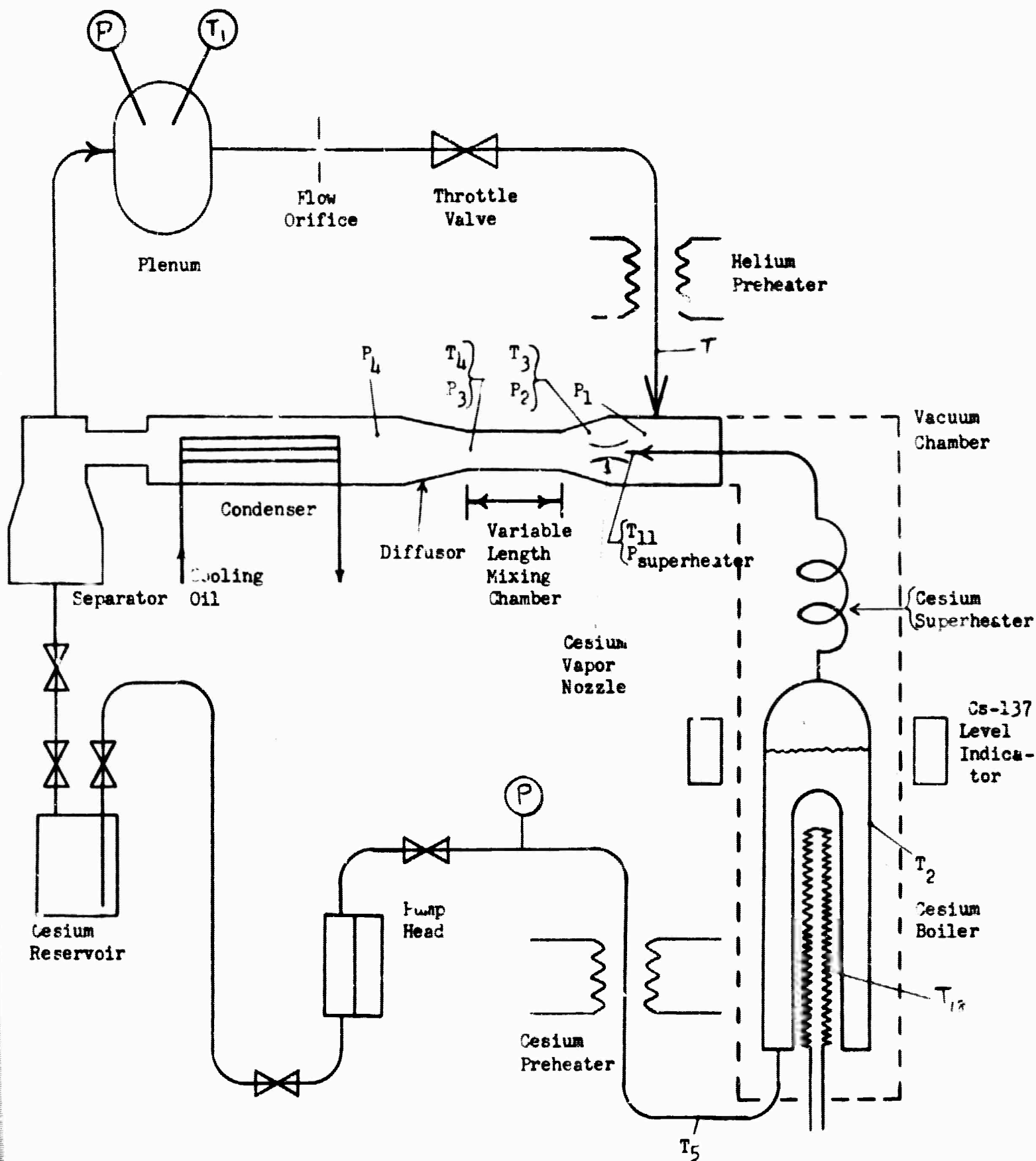


Fig. 1.

W.W.C.

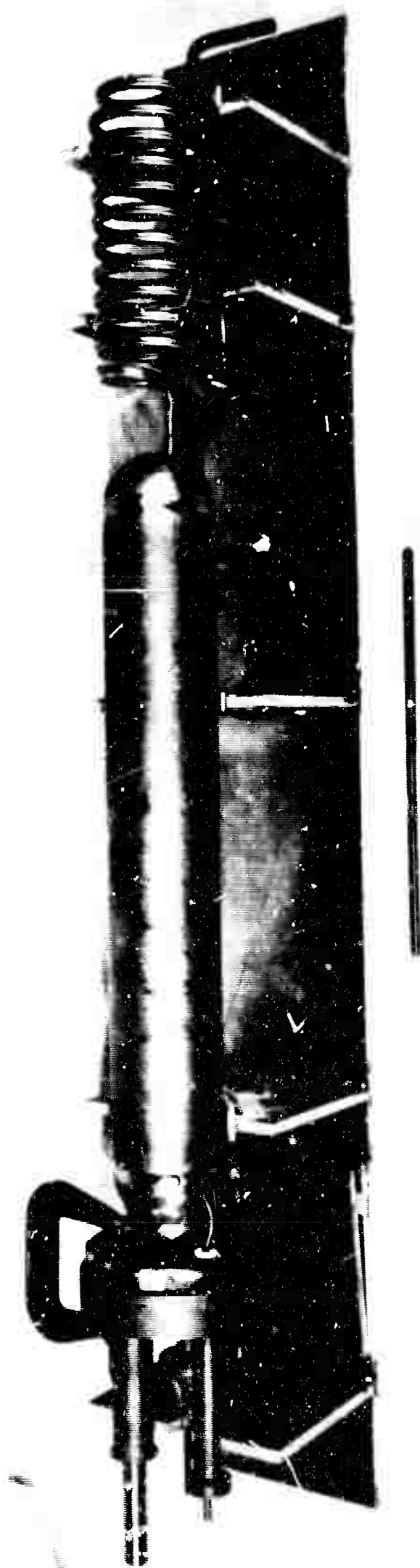


Fig. 2. Boiler (Nb-.01 Zr) and Superheater (.90 Ta-.10 W)

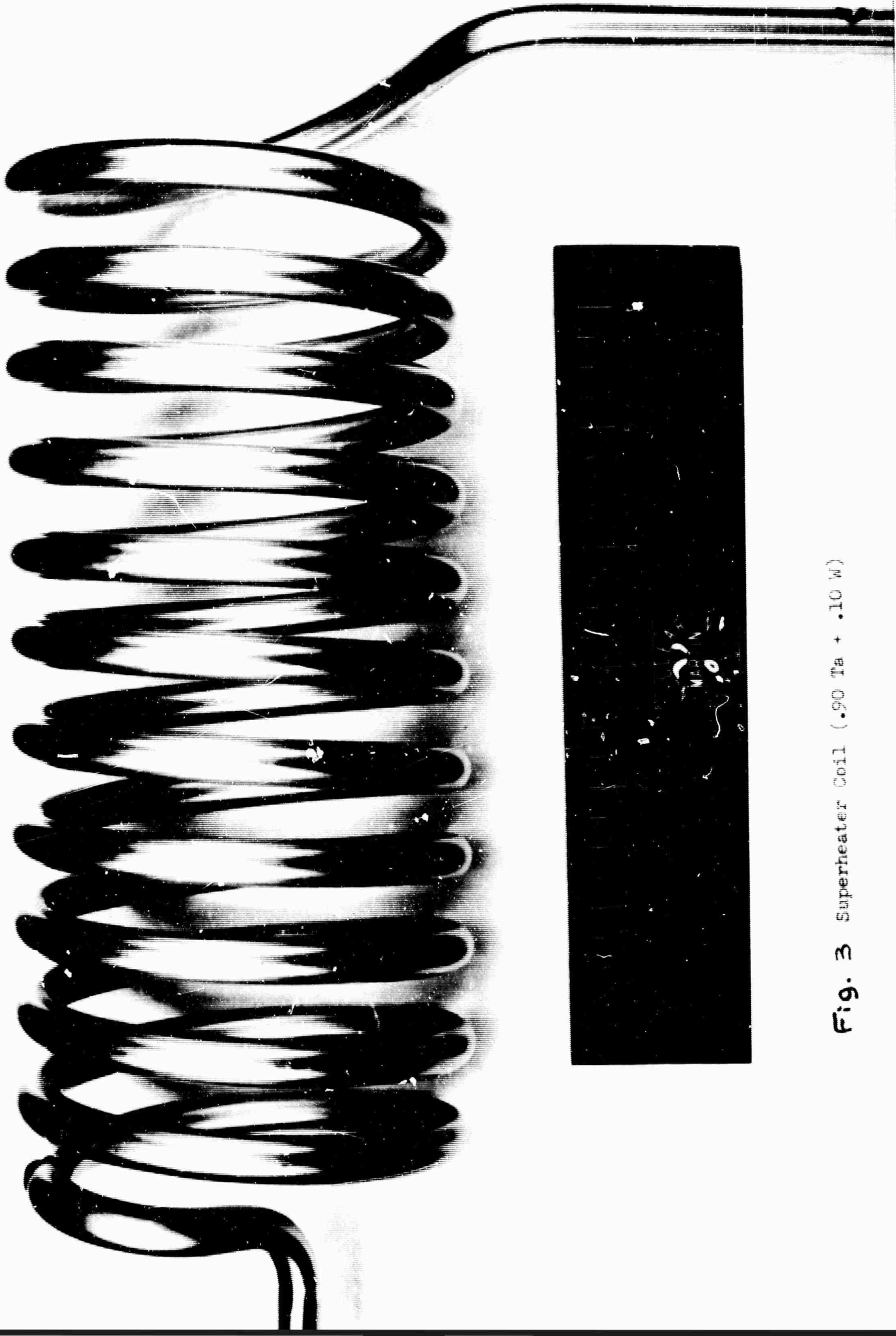


Fig. 3 Superheater Coil (.90 Ta + .10 W)

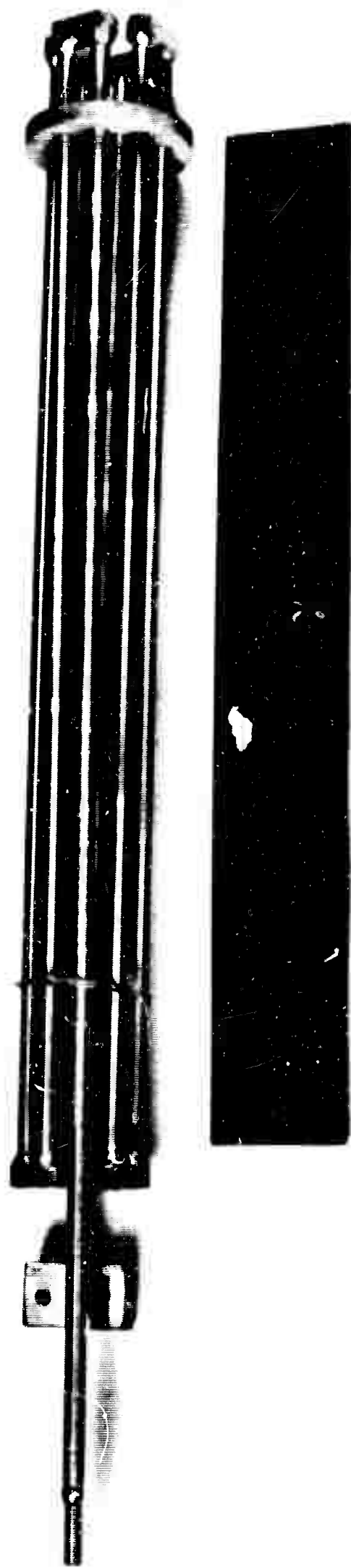


Fig. 4 Cesium Boiler Heater (Nb - 1% Zr)

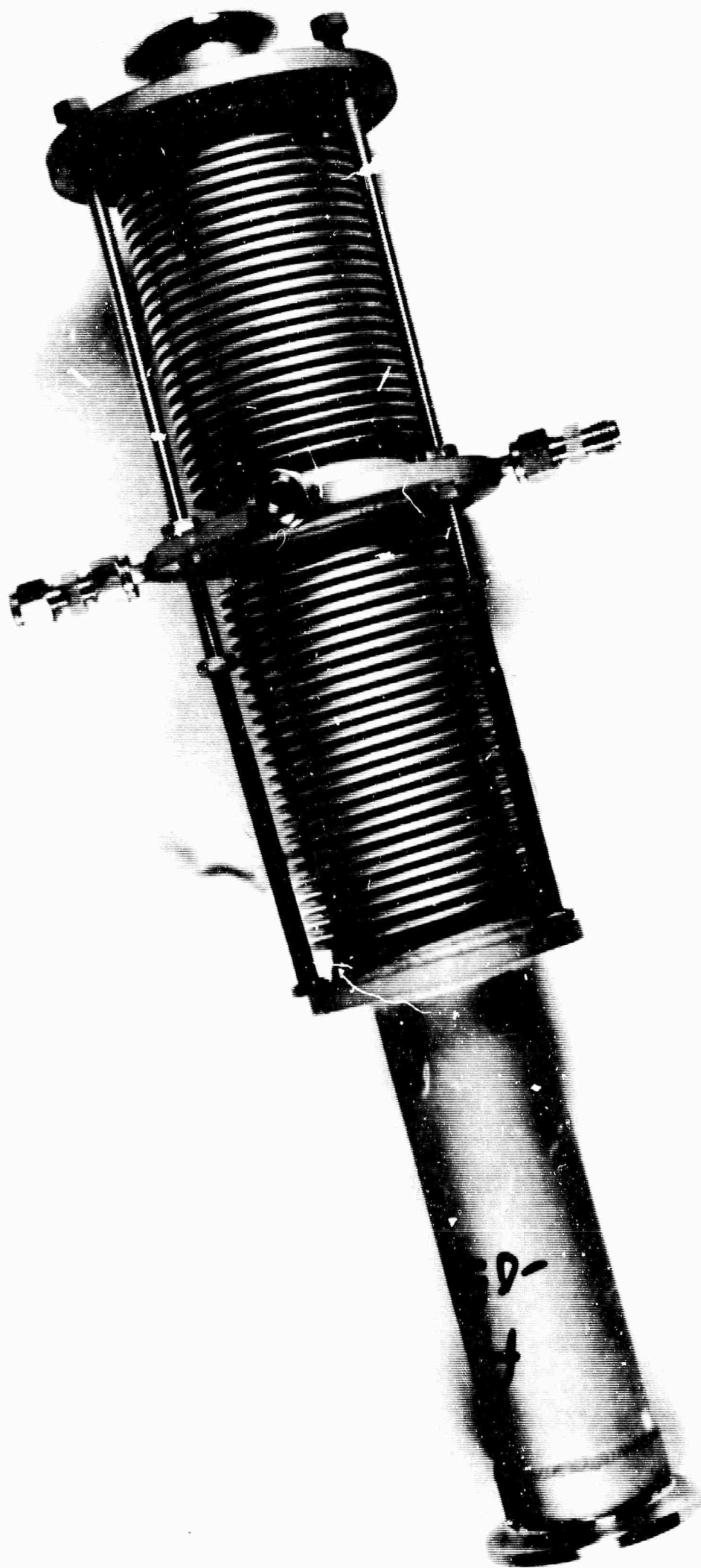


Fig. 5. Mixing Chamber (Adjustable 8½" - 12") and Diffuser

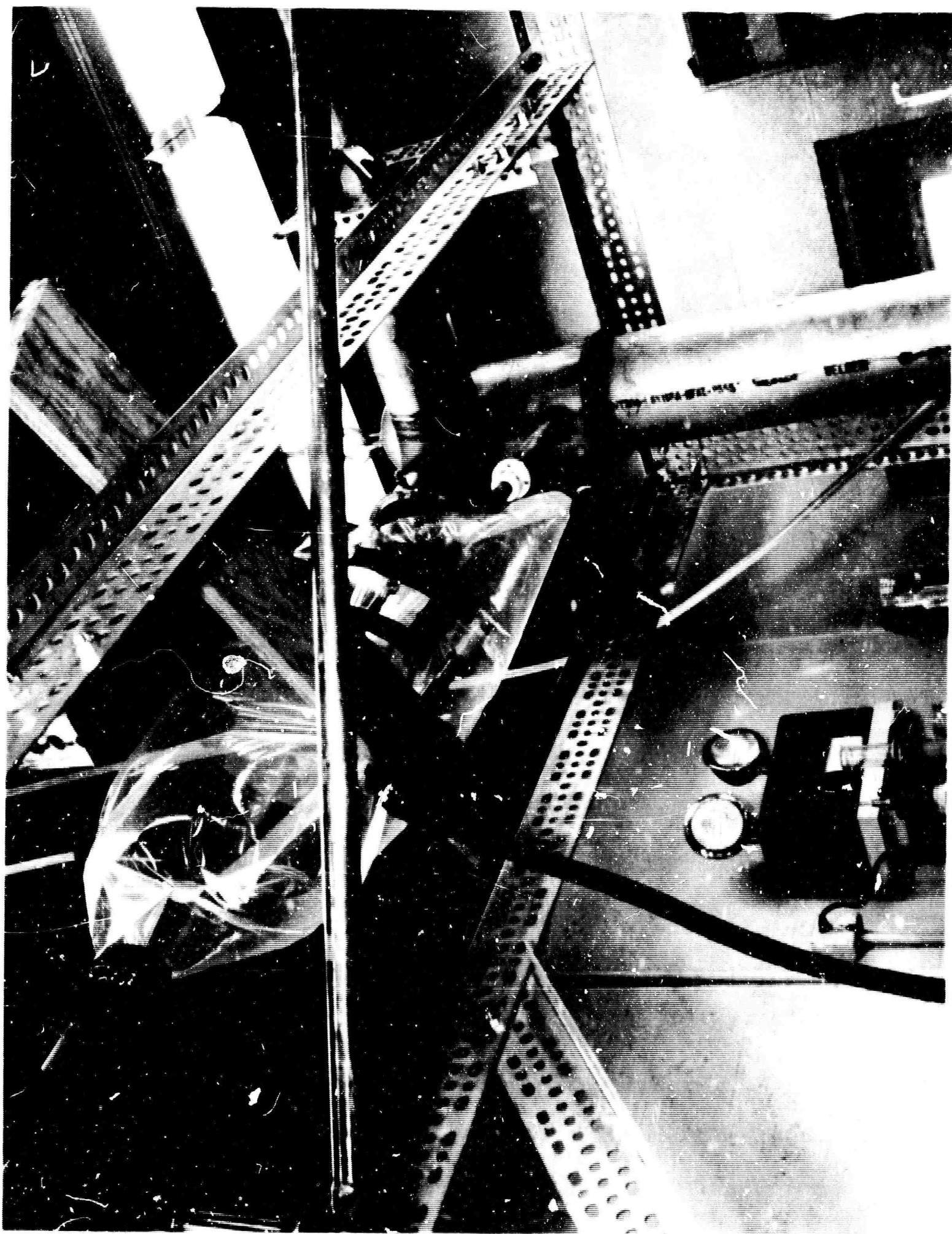


Fig. 6 Preparation for Ray-Welding Ta - .10W Primary Nozzle in Assembly

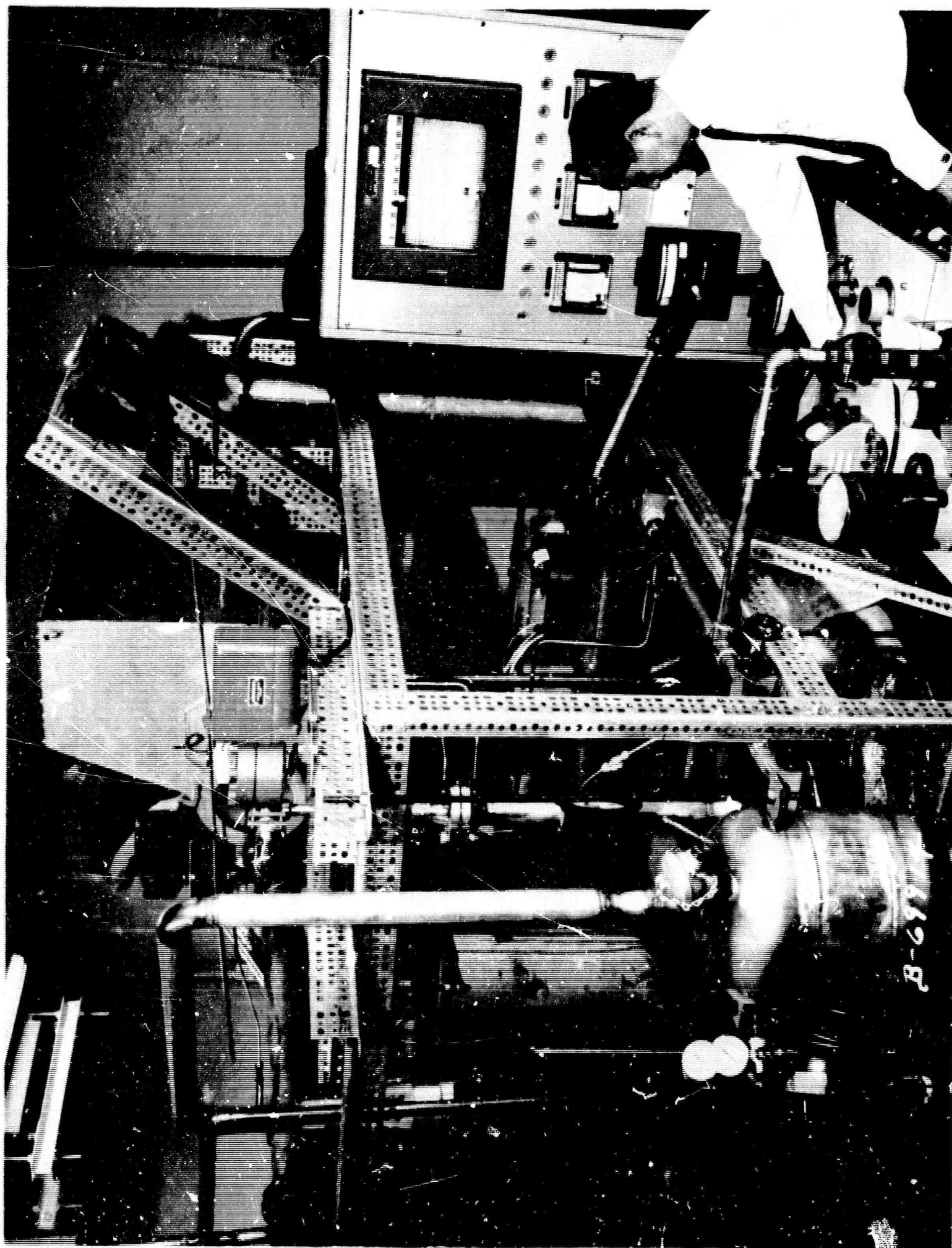
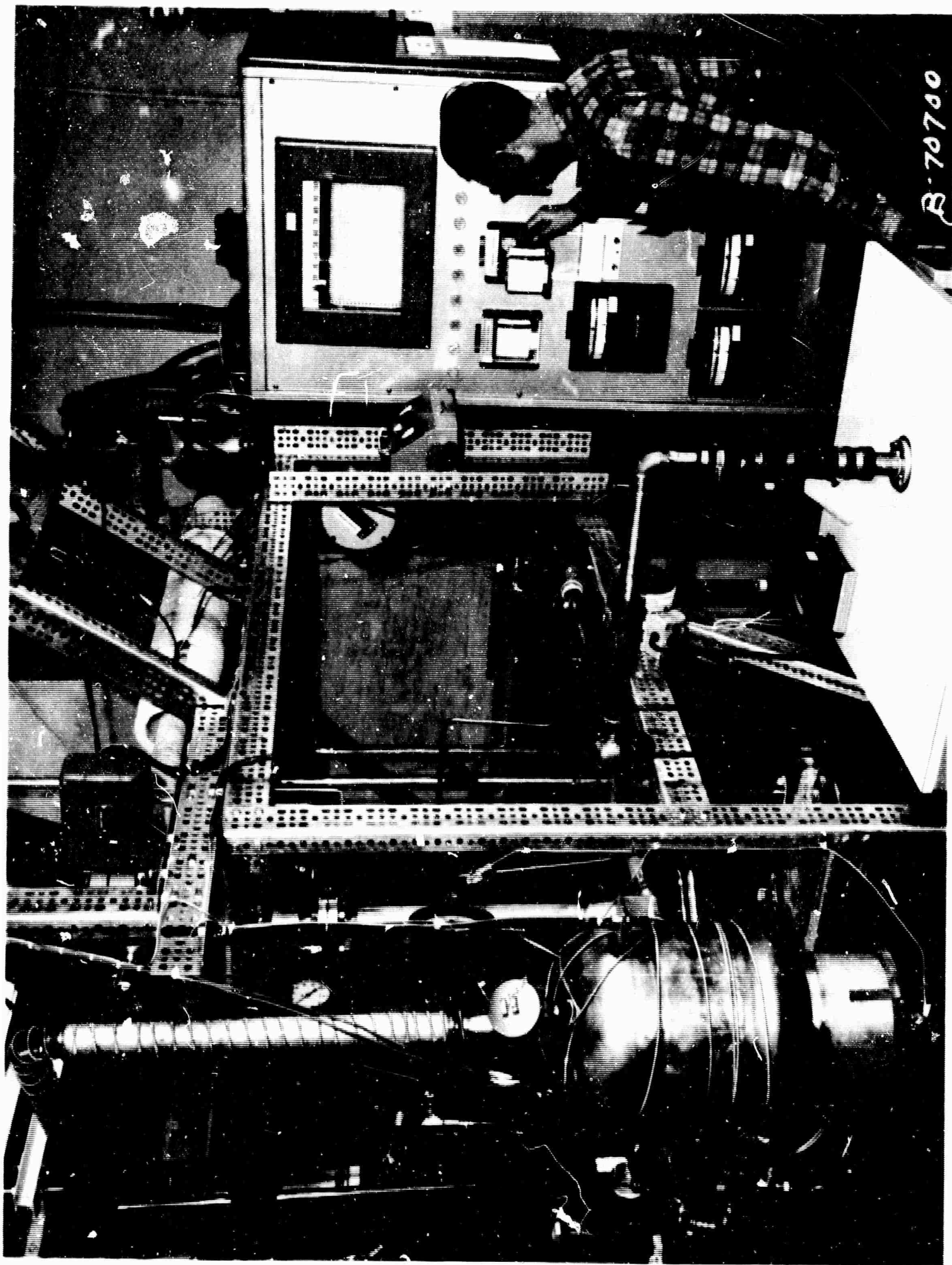
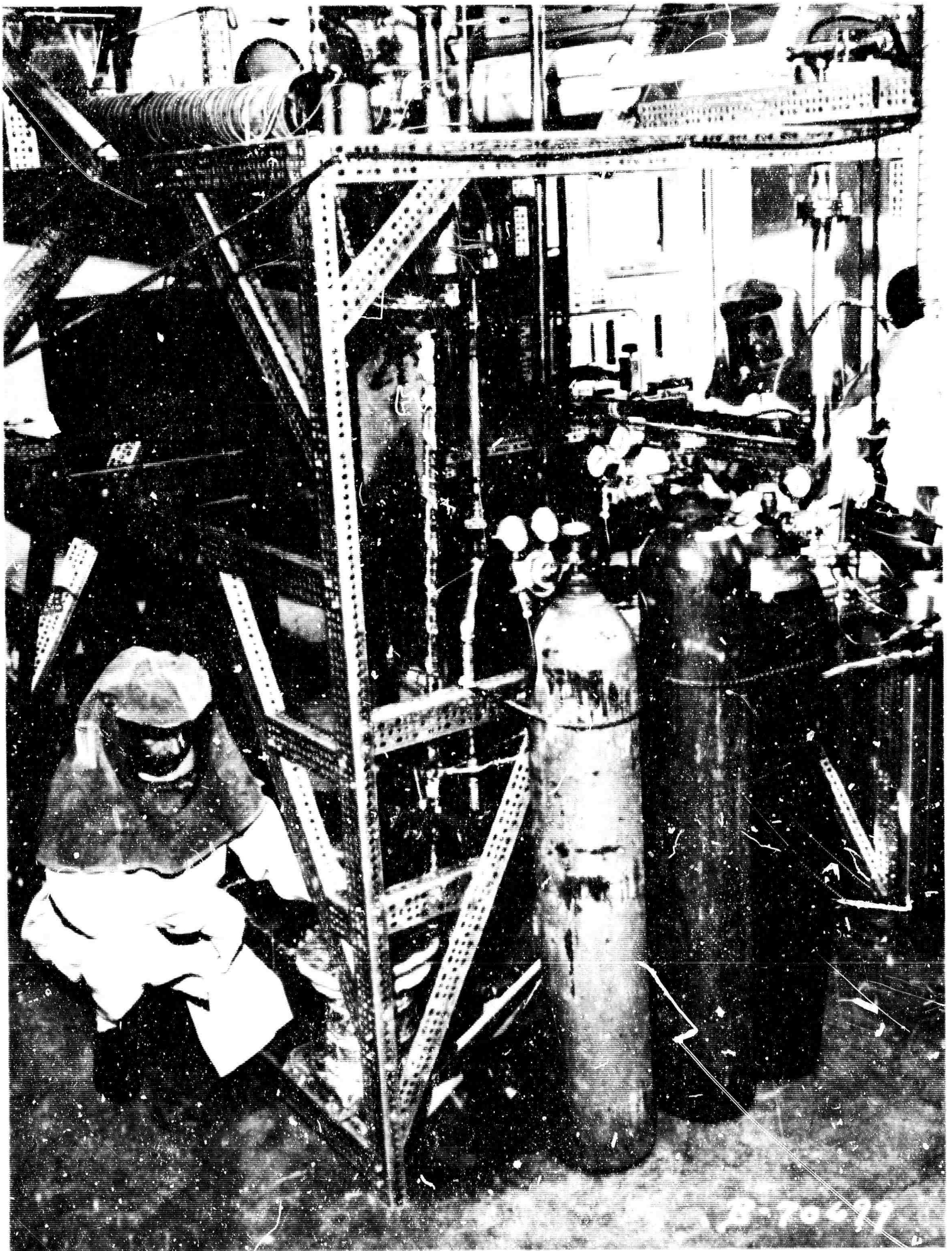


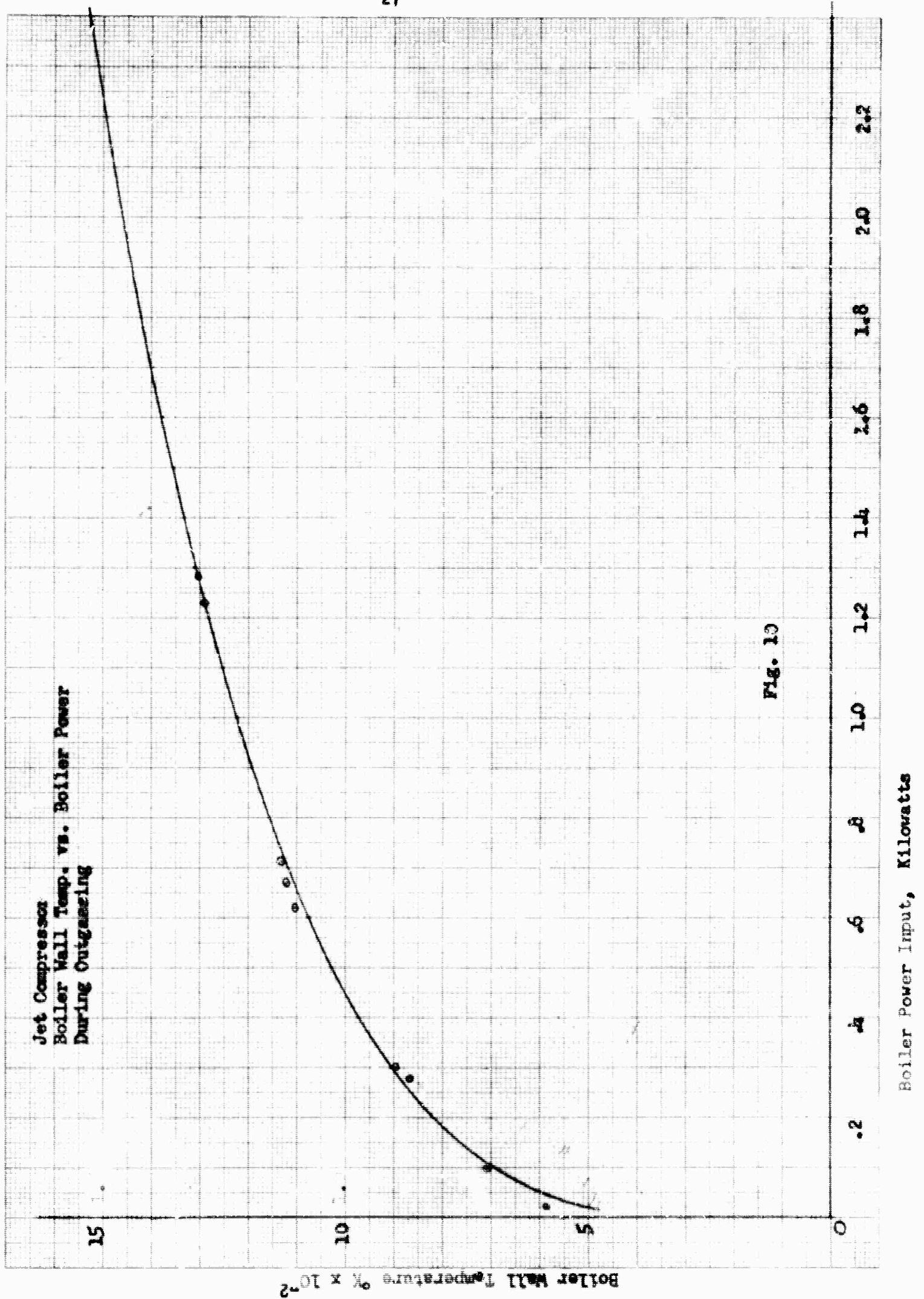
Fig. 7 System Leak Checking



B-70700

Fig 8 Calibration of Pressure Recorder





BLANK PAGE

BOILER

SUPERHEATER

RUN NO.	WALL	INPUT POWER TOTAL KW	RADIATION LOSS KW	PRESSURE	T SAT °K	HEAT OF VAPOR.	CS FLOW gm/sec		INPUT POWER KW	RADIATION LOSS KW	WALL TEMP. °K	VAPOR TEMP. °K
	T EFF °K			ATM		JOULE gm	HEAT BAL. CALN.	NOZZLE DISCHG. CALN.				
A-10	870	4.24	0.16	5.4	1160	468	6.5	5.5	2.00	1.32	1670	1575
A-11	870	4.24	0.16	5.4		468	6.5	5.5	2.00	1.32	1670	1575
A-12	930	5.29	0.44	7.4	1200	454	8.0	7.4	2.64	1.57	1690	1590
B-10	873	5.48	0.28	6.4	1180	460	8.05	7.05	1.12	.84	1400	1318

TABLE LII. RESULTS

MARTIN
-ALTIMORE

COMPRESSOR

SUPERHEATER

BOILER

BOILER										SUPERHEATER										THERMAL CYCLE										EFFECTIVENESS
RUN NO.	WALL TEMP. °K	INPUT POWER KW	RADIATION LOSS KW	PRESSURE ATM	T _{SAT} °K	HEAT OF VAPOR. JOULE/gm	HEAT BAL. CALM.		CS. FLOW gm/sec	NOZZLE DISCHG. KW	INPUT POWER KW	RADIATION LOSS KW	WALL TEMP. °K	VAPOR TEMP. °K	PRESSURE atm	HE FLOW gm/sec	HE TEMP. °K	HE DTL. PRESS. atm	INTERMEDIATE PRESSURES		PRESS. AT EXIT P ₄	PRESS. RATIO P ₄ /P ₁	COMPRESSION PWR. KW	EFFICIENCY %	THERMAL CYCLE %	EFFECTIVENESS %				
							P ₂	P ₃																						
A-10	870	4.24	0.16	5.4	1160	468	6.5	5.5	2.00	1.32	1670	1575	4.7	1.03	610	.206	.220	.254	1.23	.285	24.7	7.7	47.5							
A-11	870	4.24	0.16	5.4		468	6.5	5.5	2.00	1.32	1670	1575	4.7	.91	618	.200	.217	.244	1.30	.325	29.0	8.7	59.0							
A-12	930	5.29	0.44	7.4	1200	454	8.0	7.4	2.64	1.57	1690	1590	6.4	1.12	623	.190	.200	.260	1.37	.490	32.6	10.1	46.0							
B-10	873	5.48	0.28	6.4	1180	460	8.05	7.05	1.12	.84	1400	1318	5.5	1.48	623	.433			.483	1.12	.222	20.6	5.2	17.0						
													</																	

DATE

VI. APPENDIX

IBM 7094 PROGRAM FOR SINGLE AND 2-STAGE JET COMPRESSOR PERFORMANCE

The basic equations used in forming the Fortran code for IBM 7094 computation of jet compressor performance with both single-stage and 2-stage configurations are listed herein. The code itself is not included here, but is in storage at the Martin Company.

Primary Flow Rates*

1. Single Stage Jet Pump - The total energy available in the helium exhaust from the MHD system determines the amount of cesium that can be obtained since the energy must be used to boil and superheat the cesium for use as the pump primary fluid. The exhaust from the system under study is at 1856°K (T_e). Thus, if a 25°K temperature drop between fluids in a heat exchanger is assumed at the exit, and Mach numbers are low, the total heat available for the primary stream is:

$$Q = C_{p2} [T_e - (T_{cs} + 25)] \dot{m}_2 \quad (1)$$

where

T_{cs} = cesium saturation temperature

This heat is absorbed by the cesium on the "cold" side of the exchanger by boiling and superheating. Thus:

$$Q = \dot{m}_1 \left\{ \lambda + C_{p1} [(T_e - 25) - T_{cs}] \right\} \quad (2)$$

where λ = latent heat of vaporization per unit mass of cesium

* Analysis for one stage by C. Shih

Equating these gives:

$$\dot{m}_1 = \frac{\dot{m}_2 c_{p2} (1831 - T_{cs})}{\lambda + c_{p1} (1831 - T_{cs})}$$

The latent heat is given by:*

$$\begin{aligned} \lambda &= 5.4 \times 10^5 - 133.4 (T_{cs} - 600) \text{ joules/kg} \\ &= 6.19 \times 10^5 - 133.4 T_{cs} \end{aligned} \quad (3)$$

Also:

$$c_{p1} = 0.156 \times 10^3 \text{ joules/kg } ^\circ\text{K}$$

$$c_{p2} = 3.925 \times 10^3 \text{ joules/kg } ^\circ\text{K}$$

Substituting gives:

$$\dot{m}_1 = \frac{3.925 \times 10^3 \dot{m}_2 (1831 - T_{cs})}{9.05 \times 10^5 - 289 T_{cs}} \quad (4)$$

2. Two Stage Jet Pump - If two stages are used in the jet pump, then the following combinations can occur:

- 1) Cesium for one stage receives heat from the helium to boil and superheat it. The remaining heat is used to boil cesium and superheat it for the next stage.
- 2) Cesium for one stage is superheated to the highest possible temperature, but at a low pressure. The other stage cesium uses a portion of the remaining (lower temperature) heat for boiling and superheating. The remaining (low temperature) heat is used to boil cesium for the first mentioned stage.

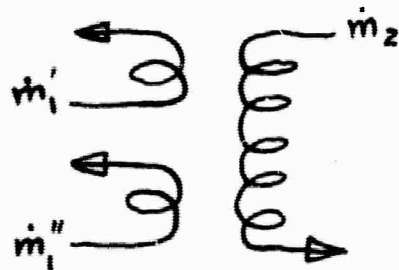
* Curve fitted to data in reference 4.

- 3) The high temperature heat is used to superheat cesium for each stage. First high pressure cesium is heated, and then lower pressure cesium. The remaining heat is utilized to boil the cesium, with the high pressure cesium produced using the higher quality heat that remains from the superheating process.

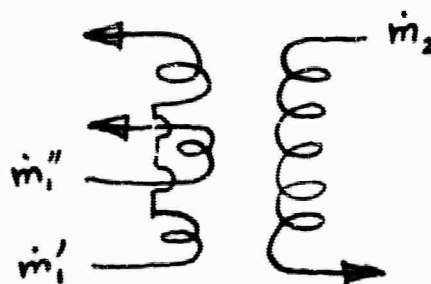
- 4) Each stage is fed from a common boiler-superheater.

The last item can be handled by merely splitting up the flow rates computed for the one stage investigation and need not be considered further here. The other possibilities may be sketched as follows:

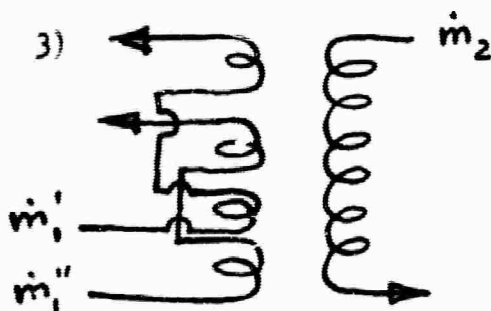
1)



2)



3)



The number of combinations is increased to six if the position of m_1' and m_1'' are reversed.

This number of combinations causes a rather interesting mess.

Consider a general type of heat exchanger where boiling only takes place:



where 5 refers to the cesium

2 refers to the helium-cesium mixture (same significance as previously)

τ = "helium" temperature

A heat balance across this system gives

$$\lambda m_5 = m_2 c_{p2} (\tau_{in b} - \tau_{out b}) \quad (5)$$

where the b subscript indicates the boiling region.

If a similar exchanger for superheating is postulated, then:

$$m_5 c_{p5} (\theta_{5in} - \theta_{5out}) = -m_2 c_{p2} (\tau_{ins} - \tau_{outs}) \quad (6)$$

where the s indicates the superheating region

θ cesium temperature.

These two equations will describe heat interchange between the two fluids under all conditions subject to the assumptions of no heat loss to the surroundings and that Mach numbers are low so that enthalpy can be equated to heat flow.

Cesium entering the superheating region will always be at the saturation temperature, which means (6) can be rewritten as

$$m_5 c_{p5} (T_{cs} - \theta_{5out}) = m_2 c_{p2} (\tau_{ins} - \tau_{outs}) \quad (7)$$

If, further, we assume the minimum temperature difference that can be attained between the cooler and hotter fluids is 25°K, and if a prime is used to refer to first stage fluid and a double prime to second stage fluid, then the following possibilities exist (see sketches of the three possible combinations):

$$\begin{aligned}
1) \quad \tau'_{ins} &= 1856^{\circ}\text{K} \\
\theta'_{5out} &= \tau'_{ins} - 25 = 1831^{\circ}\text{K} \\
\tau'_{in\ b} &= \tau'_{outs} \\
\tau''_{ins} &= \tau'_{out\ b} \\
\theta''_{5out} &= \tau''_{ins} - 25 \\
\tau''_{in\ b} &= \tau''_{outs} \\
\tau''_{out\ b} &= \tau''_{cs} + 25
\end{aligned} \tag{8}$$

$$\begin{aligned}
2) \quad \tau'_{ins} &= 1856^{\circ}\text{K} \\
\theta'_{5out} &= 1831^{\circ}\text{K} \\
\tau'_{outs} &= \tau''_{ins} \\
\tau''_{outs} &= \tau''_{in\ b} \\
\theta''_{5out} &= \tau''_{ins} - 25 \\
\tau''_{out\ b} &= \tau'_{in\ b} \\
\tau'_{out\ b} &= \tau'_{cs} + 25
\end{aligned} \tag{9}$$

$$\begin{aligned}
3) \quad \tau'_{ins} &= 1856^{\circ}\text{K} \\
\theta'_{5out} &= 1831^{\circ}\text{K} \\
\tau'_{outs} &= \tau''_{ins} \\
\tau''_{outs} &= \tau'_{in\ b} \\
\tau'_{out\ b} &= \tau''_{in\ b} \\
\tau''_{out\ b} &= \tau''_{cs} + 25 \\
\theta''_{5out} &= \tau''_{ins} - 25
\end{aligned}$$

The number of combinations is doubled if the significance of the prime is reversed.

For parametric study purposes, the helium flow rate, m_2 , will be chosen as unity, and m_5 referred to as m' or m'' , depending upon the case. Since only θ_{5out} remains, it will be referred to simply as T_I' or T_I'' , depending upon the situation. Other subscripts will be changed accordingly since the equations are now to be applied to the jet pump.

Now substitute 3 in 5:

$$(6.19 \times 10^5) - 133.4 T_{cs}) m_1 = C_{p2} (\tau_{in b} - \tau_{out b})$$

Substituting C_{p2} :

$$(157.7 - .033987 T_{cs}) m_1 = \tau_{in b} - \tau_{out b}$$

Define:

$$g_1 = 157.7 \quad (11)$$

$$g_2 = .033987$$

and we obtain:

$$(g_1 - g_2 T_{cs}) m_1 = \tau_{in b} - \tau_{out b} \quad (12)$$

Doing the same with 7 we find:

$$m_1 (T_{cs} - T_I) = -g_3 (\tau_{ins} - \tau_{outs}) \quad (13)$$

where

$$g_3 = 25.16 \quad (14)$$

Equations 12 and 13 can be written for each of the stages:

$$(g_1 - g_2 T_{cs}') m_1' = \tau_{in b}' - \tau_{out b}' \quad (15)$$

$$(g_1 - g_2 T_{cs}'') m_1'' = \tau_{in b}'' - \tau_{out b}'' \quad (16)$$

$$(T_{cs}' - T_I') m_1' = g_3 (\tau_{outs}' - \tau_{ins}') \quad (17)$$

$$(T_{cs}'' - T_I'')m_1'' = \varepsilon_3 (\tau_{outs}'' - \tau_{ins}'') \quad (18)$$

The following are common to all cases (See 8-10. Equations in boxes represent those to be solved in the order presented):

$$\boxed{\tau_{ins}' = 1856} \quad (19)$$

$$\boxed{T_I' = 1831} \quad (20)$$

$$\boxed{T_I'' = \tau_{ins}'' - 25} \quad (21)$$

From 15:

$$m_1' = \frac{\tau_{in b}' - \tau_{out b}'}{\varepsilon_1 - \varepsilon_2 T_{cs}'} \quad (22)$$

Substitute this in 17.

$$\frac{(T_{cs}' - T_I') (\tau_{in b}' - \tau_{out b}')}{\varepsilon_1 - \varepsilon_2 T_{cs}'} = \varepsilon_3 (\tau_{outs}' - \tau_{ins}') \quad (23)$$

From 16:

$$m_1'' = \frac{\tau_{in b}'' - \tau_{out b}''}{\varepsilon_1 - \varepsilon_2 T_{cs}''} \quad (24)$$

Substitute this in 18:

$$\frac{(T_{cs}'' - T_I'') (\tau_{in b}'' - \tau_{out b}'')}{\varepsilon_1 - \varepsilon_2 T_{cs}''} = \varepsilon_3 (\tau_{outs}'' - \tau_{ins}'') \quad (25)$$

One additional relationship is necessary to define the system, and can be obtained by establishing the temperature difference between primary and secondary streams at some point. The chosen difference cannot be

closer than 25°K (assumption) between the two streams.

The choice will be made at the boiler exit. Thus we obtain:

$$\text{Case 1} \quad T_{cs'} + B = \tau_{out b} \quad (26)$$

$$\text{Case 2} \quad \tau_{out b} = T_{cs''} + B \quad (27)$$

$$\text{Case 3} \quad \tau_{out b} = T_{cs'} + B \quad (28)$$

where B is a chosen constant subject to the restriction $B \geq 25$.

Now consider case 1, defined by 8 and 26. Equation 23 becomes:

$$\frac{(T_{cs'} - T_{I'}) (\tau'_{outs} - T_{cs'} - B)}{\epsilon_1 - \epsilon_2 T_{cs'}} = \epsilon_3 (\tau'_{outs} - \tau'_{ins})$$

$$\frac{T_{cs'} - T_{I'}}{\epsilon_1 - \epsilon_2 T_{cs'}} \tau'_{outs} - \epsilon_3 \tau'_{outs} = \frac{(T_{cs'} - T_{I'}) (T_{cs'} + B)}{\epsilon_1 - \epsilon_2 T_{cs'}} - \epsilon_3 \tau'_{ins}$$

$$\tau'_{outs} = \frac{(T_{cs'} - T_{I'}) (T_{cs'} + B) - (\epsilon_1 - \epsilon_2 T_{cs'}) (\epsilon_3 \tau'_{ins})}{T_{cs'} - T_{I'} - (\epsilon_1 - \epsilon_2 T_{cs'}) \epsilon_3} \quad (29)$$

$$\tau'_{in b} = \tau'_{outs} \quad (8)$$

Equation 25, 8, 26 and 21 can now be combined and written:

$$\frac{(T_{cs''} - T_{cs'} - B + 25) (\tau_{outs''} - T_{cs''} - 25)}{\epsilon_1 - \epsilon_2 T_{cs''}}$$

$$= \epsilon_3 (\tau_{outs''} - T_{cs'} - B)$$

$$\left[(T_{cs''} - T_{cs'} - B + \epsilon_5) - \epsilon_3 (\epsilon_1 - \epsilon_2 T_{cs''}) \right] \tau''_{outs} =$$

$$(T_{cs''} - T_{cs'} - B + 25)(T_{cs''} + 25) - \varepsilon_3 (\varepsilon_1 - \varepsilon_2 T_{cs''})(T_{cs'} + B)$$

$$\tau''_{outs} = \frac{(T_{cs''} - T_{cs'} - B + 25)(T_{cs''} + 25) - \varepsilon_3 (\varepsilon_1 - \varepsilon_2 T_{cs''})(T_{cs'} + B)}{T_{cs''} - T_{cs'} - B + 25 - \varepsilon_3 (\varepsilon_1 - \varepsilon_2 T_{cs''})} \quad (30)$$

$$\tau''_{ins} = \tau'_{out b} \quad (8)$$

$$T_I'' = \tau''_{ins} - 25 \quad (21)$$

$$\tau''_{in b} = \tau''_{outs} \quad (8)$$

$$\tau'_{out b} = T_{cs''} + 25 \quad (8)$$

m_1' and m_1'' follows immediately from 22 and 24.

For case 2, we have

$$\tau'_{out b} = T_{cs'} + 25 \quad (9)$$

Using 9, 25 and 27 we obtain:

$$\frac{(T_{cs''} - \tau''_{ins} + 25)(\tau''_{outs} - T_{cs''} - B)}{\varepsilon_1 - \varepsilon_2 T_{cs''}} = \varepsilon_3 (\tau''_{outs} - \tau''_{ins}) \quad (31)$$

From 9, 23 and 27 we find:

$$\tau''_{ins} = \frac{(T_{cs'} - T_I')(T_{cs''} + B - T_{cs'} - 25)}{\varepsilon_3 (\varepsilon_1 - \varepsilon_2 T_{cs'})} + \tau''_{in} \quad (32)$$

From 31:

$$\tau''_{outs} = \frac{(T_{cs''} - \tau''_{ins} + 25)(T_{cs''} + B) - \varepsilon_3 (\varepsilon_1 - \varepsilon_2 T_{cs''}) \tau''_{ins}}{T_{cs''} - \tau''_{ins} + 25 - \varepsilon_3 (\varepsilon_1 - \varepsilon_2 T_{cs''})} \quad (33)$$

$$\tau_{outs'} = \tau_{ins''}$$

$$\tau_{in b}'' = \tau_{outs}''$$

$$T_I'' = \tau_{ins''} - 25$$

$$\tau_{in b}' = \tau_{out b}''$$

(9)

m_1' and m_1'' follow from 22 and 24.

For case 3 we have equation 28 and:

$$\tau_{out b}'' = T_{cs}'' + 25$$

(10)

$$\tau_{in b}'' = \tau_{out b}'$$

(10)

From 23 and 10:

$$\frac{(T_{cs}' - T_I')(\tau_{outs}'' - \tau_{out b}')}{\varepsilon_1 - \varepsilon_2 T_{cs}'} = (\tau_{ins}'' - \tau_{ins}') \varepsilon_3$$

$$\tau_{ins}'' = \tau_{ins}' + \frac{(T_{cs}' - T_I')(\tau_{outs}'' - \tau_{out b}')}{\varepsilon_3 (\varepsilon_1 - \varepsilon_2 T_{cs}')} \quad (34)$$

From 25 and 10

$$\frac{(T_{cs}'' - \tau_{ins}'' + 25)(\tau_{in b}'' - \tau_{out b}'')}{\varepsilon_1 - \varepsilon_2 T_{cs}''} = \varepsilon_3 (\tau_{outs}'' - \tau_{ins}'')$$

$$\tau_{ins}'' = \frac{\varepsilon_3 (\varepsilon_1 - \varepsilon_2 T_{cs}'') \tau_{outs}'' - (T_{cs}'' + 25)(\tau_{in b}'' - \tau_{out b}'')}{\varepsilon_3 (\varepsilon_1 - \varepsilon_2 T_{cs}'') - (\tau_{in b}'' - \tau_{out b}'')} \quad (35)$$

Now equate 35 and 24:

$$\tau'_{ins} + \frac{(T_{cs'} - T_{I'}) (\tau''_{outs} - \tau'_{out b})}{\epsilon_3 (\epsilon_1 - \epsilon_2 T_{cs'})} =$$

$$\frac{\epsilon_3 (\epsilon_1 - \epsilon_2 T_{cs''}) \tau''_{outs} - (T_{cs''} + 25) (\tau''_{in b} - \tau''_{out b})}{\epsilon_3 (\epsilon_1 - \epsilon_2 T_{cs''}) - (\tau''_{in b} - \tau''_{out b})}$$

$$\frac{T_{cs'} - T_{I'}}{\epsilon_3 (\epsilon_1 - \epsilon_2 T_{cs'})} \tau''_{outs} = \frac{\epsilon_3 (\epsilon_1 - \epsilon_2 T_{cs''}) \tau''_{outs}}{\epsilon_3 (\epsilon_1 - \epsilon_2 T_{cs''}) - (\tau''_{in b} - \tau''_{out b})}$$

$$= -\tau'_{ins} + \frac{T_{cs'} - T_{I'}}{\epsilon_3 (\epsilon_1 - \epsilon_2 T_{cs'})} \tau'_{out b} -$$

$$- \frac{(T_{cs''} + 25) (\tau''_{in b} - \tau''_{out b})}{\epsilon_3 (\epsilon_1 - \epsilon_2 T_{cs''}) - (\tau''_{in b} - \tau''_{out b})}$$

$$\tau''_{outs} = \frac{-\tau'_{ins} + \frac{T_{cs'} - T_{I'}}{\epsilon_3 (\epsilon_1 - \epsilon_2 T_{cs'})} \tau'_{out b} - \frac{(T_{cs''} + 25) (\tau''_{in b} - \tau''_{out b})}{\epsilon_3 (\epsilon_1 - \epsilon_2 T_{cs''}) - (\tau''_{in b} - \tau''_{out b})}}{\frac{T_{cs'} - T_{I'}}{\epsilon_3 (\epsilon_1 - \epsilon_2 T_{cs'})} - \frac{\epsilon_3 (\epsilon_1 - \epsilon_2 T_{cs''})}{\epsilon_3 (\epsilon_1 - \epsilon_2 T_{cs''}) - (\tau''_{in b} - \tau''_{out b})}}$$

τ''_{ins} can now be found from

35

Then

$$\tau'_{outs} = \tau''_{ins} \quad (10)$$

$$\tau'_{in b} = \tau''_{out s} \quad (10)$$

and m_1' and m_1'' follow from 22 and 24.

BIBLIOGRAPHY OF REFERENCES

1. Martin Company Semi-Annual Technical Summary Report on Research Program on Application of Jet Compressor to MPD Electrical Power Generation, MND-3124, January 1964.
2. C. Shih, "A Study of Closed Cycle MPD Power Generator Compatible with Jet Compression," Proceedings of the International Symposium of MHD Electrical Power Generation, July 1964, Paris, France.
3. S. S. Eichacker & H. Hoge "Jet Compressor Efficiency as Influenced by the Nature of the Driving and Driven Gases," August 1960, Journal of the Aero Space Sciences, V. 27, No. 8.
4. W. O. Weatherford, Jr., J. C. Tyler and P. M. Ku, "Properties of Inorganic Energy Conversion and Heat Transfer Fluids for Space Application," Southwest Research Institute, WADD Technical Report 61-96.

DISTRIBUTION LIST

	<u>No. Copies</u>
Office of Naval Research Power Branch (Code 429) Washington, D. C. 20360 Attn: John A. Satkowski	6
Commanding Officer Office of Naval Research Branch Office Box 39 Navy #100 Fleet Post Office New York, New York	1
Chief, Bureau of Ships Washington, D. C. 20360 Attn: Dr. John Huth Chief Scientist	1
U. S. Naval Research Laboratory Washington, D. C. 20390 Attn: Technical Information Division	6
Director Advanced Research Projects Agency Material Sciences Division Washington, D. C. 20301	1
Wright-Patterson Air Force Base Aeronautical Systems Division Ohio Attn: Don Warnock (ASRMFP-2)	1
Air Force Office of Scientific Research Washington 25, D. C. Attn: Dr. Milton M. Slawsky	1
U. S. Naval Ordnance Test Station Propulsion Applied Research Group China Lake, California Attn: Mr. Leroy J. Krzycki (Code 4506)	1
Army Natick Laboratory Pioneering Research Division Natick, Massachusetts Attn: Mr. Harold J. Hoge	1

Rome Air Development Center Rome, New York Attn: Mr. Frank J. Mellura	1
U. S. Naval Ordnance Laboratory NA Division White Oak, Maryland Attn: Wallace Knutsen Library	1 2
Defense Documentation Center Cameron Street Alexandria, Virginia 22314	20
U. S. Army Research & Development Laboratory Fort Belvoir, Virginia Attn: Frank Shields (ERD-EP)	1
National Aeronautics and Space Administration Lewis Research Center 21000 Brookpark Road Cleveland 35, Ohio Attn: John Stevens Dr. B. Lubarsky	1 1
U. S. Atomic Energy Commission Division of Reactor Development Direct Energy Conversion Section, RD; AED Germantown, Maryland	1
Dr. T. Brogan AVCO-Everett Research Laboratory 2385 Revere Beach Parkway Everett, Massachusetts	1
Dr. B. Zauderer General Electric Company Valley Forge Space Technical Center Philadelphia 1, Pennsylvania	1
Dr. M. E. Talaat Department of Mechanical Engineering University of Maryland College Park, Maryland	1

Dr. W. D. Jackson Electrical Engineering Department Massachusetts Institute of Technology Cambridge 39, Massachusetts	1
Dr. B. C. Lindley Nuclear Research Centre C. A. Parsons & Company, Ltd. Fossway, Newcastle Upon Tyne 6 England	1
Dr. Robert Eustis Thermosciences Division Stanford University Stanford, California	1
Dr. Richard Schamberg Rand Corporation 1700 S. Main Street Santa Monica, California	1
Dr. W. S. Emmerich Westinghouse Research Laboratories Beulah Road, Churchill Borough Pittsburgh 35, Pennsylvania	1
Dr. R. T. Schneider Allison Division General Motors Corporation Indianapolis, Indiana	1
Dr. D. G. Elliott Jet Propulsion Laboratory Pasadena, California	1
Dr. Phil Hill Department of Mechanical Engineering Massachusetts Institute of Technology Cambridge, Massachusetts 02139	1
Dr. John J. Connelly, Jr. State University of New York College at Fredonia Physics Department Fredonia, New York 14063	1